Tuijin Jishu/Journal of Propulsion Technology
ISSN: 1001-4055
Vol. 45 No. 4 (2024)

Dynamic Response Analysis of Two Different Cable-Stayed Bridge Using Blast Load

Rina Kumari [1], Prof S. S Mishra [2]

Research scholar[1], Department of Civil Engineering, N.I.T Patna

Professor[2] Department of Civil Engineering, N.I.T Patna

Abstract:
This study focused on the dynamic response and progressive collapse behavior of cable-stayed bridges subjected to blast load on H-type pylon with different cable arrangements (fan, radial). Using advanced computational simulations, this study aims to provide insights for optimizing bridge designs and enhancing resilience against blast-induced effects. This study utilizes ETAB, FEM analysis to assess the time period and frequency behavior of fan and radial type cable arrangements in cable-stayed bridges, displacement and drift of structural member subjected to blast loading conditions. The study underscores the structural efficacy of specific cable arrangements, identifying the FAN arrangement with an H-type pylon exhibits better resistance against blast loading.

Keywords: *Blast load, ETAB, Dynamic response, Progressive collapse, Cable stayed bridge*

1. Introduction

The socio - economic growth of any country depends upon its various means of transportation and bridges play a lifeline system for transportation. Bridges are one of the most expensive structures and always prone to various blast loads either blast from accidental collision or terrorist attack during its service life. Therefore, these bridges require to safeguard against blast loadings. Explosive materials are extensively used in military for demolition work, construction and development works [1] which have great efficiency to damage structures. A lot of investigation has been conducted on cable-stayed and suspension bridges considering earthquakes and wind loads still need more attention by the researchers to accidental and explosion loading on the structures. The literatures based on blast loadings are mostly focused on reinforced concrete and steel structure of buildings. A very few researchers have studied the analysis of bridges under the blast loading and therefore still needs investigation [2]. The existing guidelines for blast resistant bridge design are restricted only for some particular structural component [3] and therefore it is very necessary for researchers to examined the response pattern of bridge components like deck, pier and pylons under various dynamic loading.

Bridges are more vulnerable against extreme loading conditions than buildings because bridges have less structural redundancy as compared to buildings. Thus, in the case of the failure of any primary structural members in bridges, redistribution of the applied load through alternative load paths to prevent potential progressive collapse is almost impossible [4-6]. Moreover, the residual load carrying capacity of the supporting elements is critical for global stability as well as safety for occupants [7].

Identifying the vulnerable parts and potential cable loss scenarios and realizing the form and extent of the damage of the deck and pylons can be the first step towards comprehending the behavior of cable-stayed bridges subjected to explosions, and developing appropriate mitigation strategies.

2. Literature Review

The finite element (FE) was conducted by Son et al. [2011] to evaluate the response of a hollow steel box pylon of a cable-stayed bridge subjected to blast loading [9]. The interaction between the air blast and pylon using an Arbitrary Lagrangian Eulerian (ALE) method. In the FE model, the cables were not modeled and only the corresponding forces were applied and assumed to be constant throughout model. The FE analysis results shows that the P-D effects causing significant instability in the hollow steel box pylons under the blast loadings. They concluded that that the concrete infilled pylons perform better as compare to conventional pylon.

Winget et al. [2005] sum up all the ongoing research work to evolve performance-based blast design standards for bridges and also explained the probable effect of blast load on bridges and to minimize these effects also suggest retrofit and structural design solutions [2].

Pan et al. [2017] explore three different types of bridge like RC bridge, slab on girder bridge and long span cable bridge under several blast load condition and discussed their global and localized damage response of the structure [11].

Cofer et al. [2012] made a FE model of a precast and prestressed concrete girder bridge and verify them by performing two blast load tests. At mid span of the bridge three different blast load cases on, above and below the deck and when load applied below the deck slab damaged severely but girder remain safe. Other two blast load cases applied on and above the deck exhibits severe local damage but there was also a probability to restart the other part of the bridge just after the blast incident [12].

Tabar et al. [2019-20] observed the cable-stayed bridges under earthquake and found that for bridges like cable stayed bridges which is having expensive construction costs should be designed and analyzed to resist extreme loading conditions like blast load [13-15].

C.D et al. [2019] examined cable-stayed bridge using large scale numerical analysis by applying blast load and concluded the failure mechanism of generic cable-stayed bridge by performing nonlinear analysis to observe the ultimate resisting capacity of blast load and through simulation explained damage induced due to the dynamic response [16].

Son and Lee [2011] explored the blast resistance performance of two different types of pylons like concrete-filled composite pylon and hollow steel box pylon of cable-stayed bridge and then studied the damage patterns of the pylon. They found the better resistance performance of concrete-filled composite pylon over the hollow steel box type pylon [9].

Shukla and Modhera [2015] have conducted FE analysis using SAP2000 software for the investigation of Surat city, Gujarat, India based cable-stayed bridge model under blast loading [17].

Kanafani et al. [2010] determined blast induced pressure at different elevation of pylon using TM 5-1300 and then transformed its into quasi-static blast loading condition and compared maximum bending moment, shear force at various standoff distances through multiple graphs [3].

Tang and Hao et al. [2010] performed a numerical research work on cable-stayed bridge's deck, pier and tower's damage mechanism and its damage intensity through simulation [10].

Hashemi et al. [2016] examined dynamic response of cable-stayed bridge subjected to blast load and evaluate the potential progressive collapse under different blast loading condition by using FE simulation [18]. Redundancy in the structural design of the bridge has been demonstrated to be a critical strategy for mitigating disproportionate collapse. This type of collapse occurs when a localized failure triggered by a small event propagates to other structural elements, resulting in the collapse of the entire structure. This phenomenon is commonly known as progressive collapse, wherein the failure progressively spreads from one member to another until a significant portion or the entirety of the structure collapses.

Domaneschi et al. [2020] through a numerical progressive collapse analysis using the Applied Element Method (AEM) investigated the collapse Morandi's Polcevera viaduct and identified fatigue, corrosion, insufficient redundancy and construction errors as the primary causes of the collapse [19].

Domaneschi et al. [2018] studied the disproportionate collapse of an existing cable-stayed bridge and explore an alternative structural configuration as a potential solution to enhance the bridges response. This alternative scheme aimed to establish different loading path to mitigate disproportionate collapse effectively [20].

G. et al. [2020] performed numerical analysis for investigation of progressive collapse due to collision between ship and the pier of cable stayed bridge [21].

Tang and Hao et.al. [2010] performed numerical analysis using LS-DYNA a FE software to study the dynamic behavior of a RC cable-stayed bridge subjected to blast load and after that observed the response analysis of CFRP strengthened deck and found that use of CFRP was not effective in minimizing the blast induced damage of the deck [10, 22].

Deng and Jin et al. [2009] have studied the dynamic response of a cable-stayed bridge subjected to blast loading. They concluded that the explosion can lead to localized destruction of the deck in the vicinity of the detonation [23].

3. Methodology

The methodology for the study of the cable-stayed bridge involves a sequential process encompassing various stages explained with flow chart (Figure 1). The initial stage involves the utilization of ETAB modeling software to create a detailed and accurate representation of the cable-stayed bridge. This modeling process incorporates the gathered data and accounts for the dynamic interactions between the various components of the structure. The ETAB model serves as a virtual platform for simulating different loading conditions and assessing the bridge's performance under various scenarios. Following the modeling phase, the study progresses to the analysis of results and subsequent discussions. This step involves the interpretation of data obtained from the simulations and the comparison of performance metrics under different conditions. This comprehensive methodology ensures a systematic and thorough exploration of the bridge's dynamic response to blast loads and the potential for progressive collapse, contributing valuable insights to the field of structural engineering. This involves an examination of how the structure responds to dynamic loads generated by blast events, considering the potential impact on its integrity. Finally, the methodology concludes with the formulation of conclusive remarks and recommendations.

To understand and analyze blast load for cable stayed bridge is more complicated and difficult. In this study blast load are converted into an equivalent static load to simplify their calculation and analysis. The analysis focused on the behavior of a cable-stayed bridge subjected to an assumed blast load magnitude. A specific blast location was selected, and its impact on the structure was evaluated. Figure 2 illustrates a typical force-deformation curve, with line AB depicting linear elastic behavior. The slope from point A to B signifies the effective elastic stiffness of the member

until yield (point B), beyond which plastic hinge deformation begins. Line BC represents strain hardening, with the slope from B TO C typically set to ensure the ultimate capacity at point C is 0-10% higher than the yield capacity. Point CD indicates initial failure, while line DE shows the members residual strength, with point E marking failure.

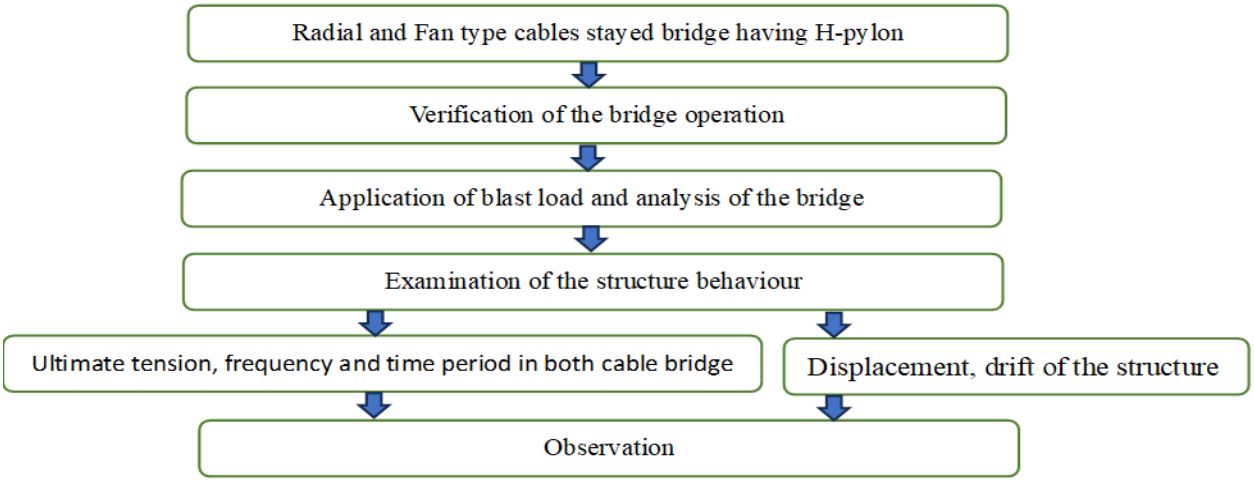

Figure 1: Methodology of Work

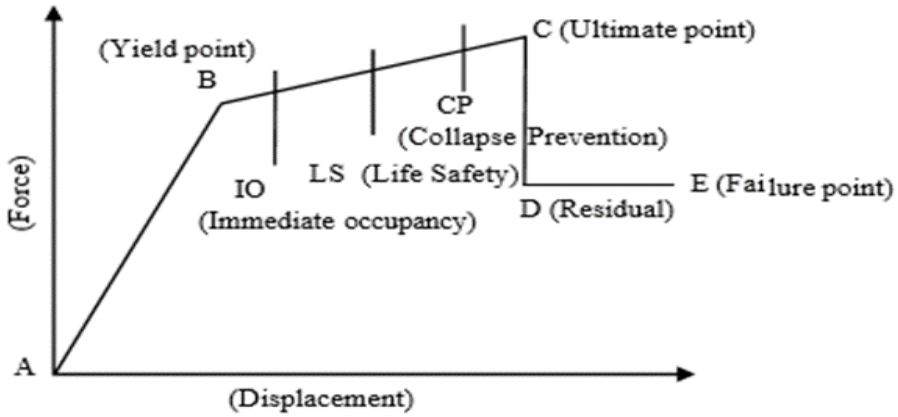

Figure 2: force – displacement curve [ASCE 41-17]

3.1 Bridge details

The target cable-stayed bridge features two end spans with a single pylon. The decision on this configuration was informed by a comprehensive study of various cable-stayed bridges constructed both in India and abroad. The bridge's design with a total length of 240 meters, two end spans, each measuring 120 meters, and a single tower standing at a height of 40 meters below the deck and 60 meters above the deck. The tower section is specified as 5m x 5m. The bridge deck has a width of 26.5 meters, accommodating six lanes and two pedestrian tracks. The girder, assumed to

be hinged with the tower at a height of 40 meters above the base and simply supported at both ends, features a depth of 3 meters. The schematic diagram in Figure 3. illustrates the bridge's single tower, 100 meters in height, and two equal end spans of 120 meters. The girder is supported by a total of 28 stay cables, 14 on each side, with a spacing of 17 meters. The tower's cross-section is specified as 5m x 5m. The box girder is characterized by a thickness of 0.2 meters and side thickness of 0.3 meters. The yield axial force of a cable is determined to be 3312 kN based on material and cross-sectional properties. This design aims to optimize structural stability and functionality for the cable-stayed bridge.

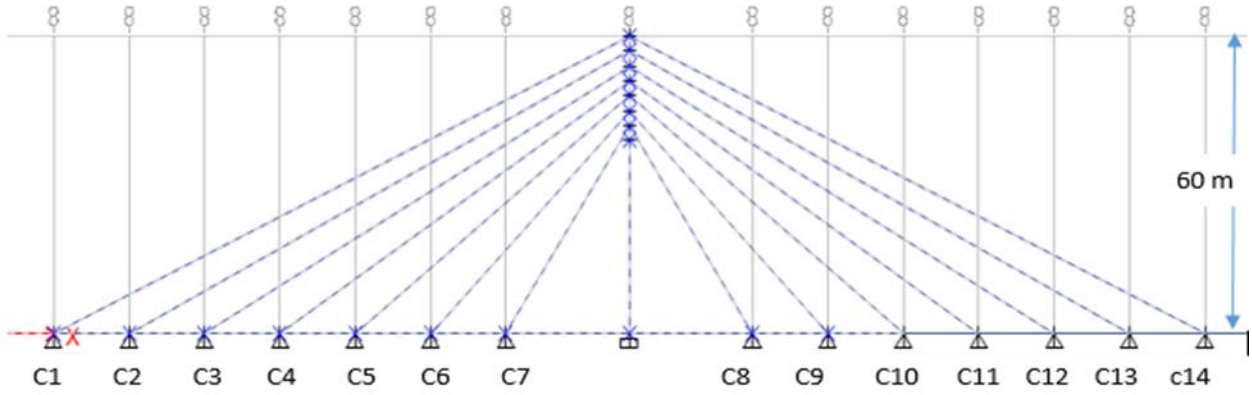

Figure 3: Geometry of the target Cable-stayed bridge

3.2 Cables:

Cables are seven wire high tensile strength strands bound together in a hexagonal shape. They are galvanized and sheathed with a tight high density polyethylene coating to protect against corrosion. The cables have passive connections to the tower and an active connection to the girder. Figure 4 shows the typical cross-section of cables.

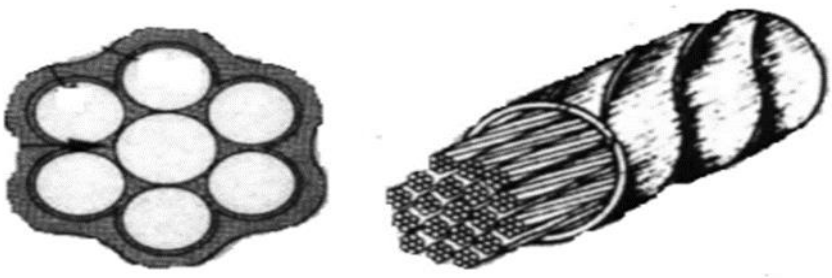

Figure 4: Cable cross-section

3.3 Pylon:

The bridge has H-shaped pylon and it has 60 m height above the deck and 40 m below the deck elevation. Pylon’s upper portion is reinforced with a steel plate where the cables are anchored. Cable-stayed bridge pylon is made of concrete and having box like cross -section.

3.4 Material Properties:

The materials employed in the construction of the cable-stayed bridge encompass concrete and steel for specific components. The reinforced pylon and box girder utilize concrete with the following properties. For the cables, steel is employed with distinct properties. These material specifications are crucial considerations in ensuring the structural integrity and performance of the cable-stayed bridge, with each component designed to meet the required standards for strength, elasticity, and density.

Table 1: Concrete Properties

Grade of the concrete	M40
Modulus of Elasticity	3.16×10^7 N/mm^2
Poison's ratio	0.2
Weight density	22.241 KN /m^3

Table 2: Steel Properties

Ultimate Strength	1860 KN/m^2
Modulus of Elasticity	2.0×10^8 N/mm^2
Poison's ratio	0.3
Weight density	76.98 KN/m^3

3.5 3D Modeling of the bridge

ETAB is the easiest way to achieve productive solution for various design requirements and for their structural analysis. This software can analyzed simple 2D frames as well as very complex 3D structures. It is the most suitable FE tool for modelling and progressive collapse analysis of cable-stayed bridges. The two types of cable arrangements e.g fan and radial cable patterns have been modelled using ETAB as shown in following Figures 5&6.

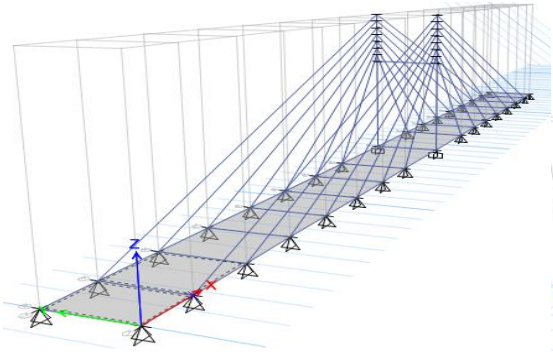

Figure 5: Fan Cable arrangement

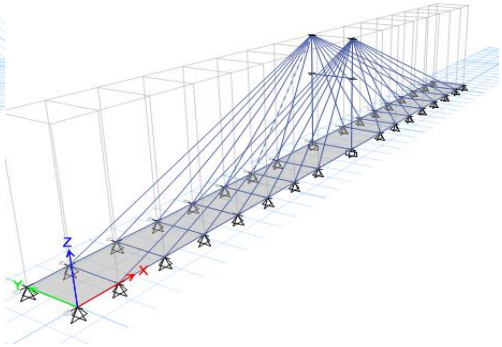

Figure 6: Radial Cable arrangement

4. Result & Discussion

The analysis of deflection of girder and axial cable forces for various combinations of cable arrangements and geometry of pylon are discussed below.

4.1 Analysis of Deflection of Girder

The analysis of deflection or the vertical displacement of girder is one of the most significant criteria while the analysis of bridges is considered. The analysis is done for the two different arrangements of cable with H - type of pylon and the maximum deflection of girder is calculated subjected to blast load.

4.2 Blast Load Calculation

Blast load analysis is a critical process used in structural engineering to assess the effects of explosions on buildings, infrastructure, and other constructed elements. This analysis evolves the dynamic response of structures subjected to the sudden release of energy generated by an explosion. Engineers utilize sophisticated computational models to simulate the blast wave propagation, structural deformation, and potential failure mechanisms. By considering factors such as blast intensity, duration, and distance from the explosion source, engineers can estimate the forces exerted on various structural components and assess their ability to withstand such loads. Blast load analysis plays a crucial role in designing resilient structures for both civilian and military applications, aiming to minimize casualties, property damage, and disruption to critical infrastructure in the event of an explosion.

Blast loads are complex in nature. Using TM 5-1300 for computational simplification and to reduce analysis time, blast loading is typically converted into an equivalent static load. The amount of total blast pressure is inversely proportional to the scaled distance (Z) as per TM 5-1300 is given in Eq. (1).

$$\boldsymbol{Z} = \frac{\boldsymbol{R}}{\boldsymbol{W^{1/3}}} \qquad \text{…. (1)}$$

The equation for blast load scaled distance, represents a fundamental concept in blast engineering. Here, R is the radial distance from the point of explosion to the different requirement points (in meters), and W is the weight of the explosive charge (in L).

In simpler terms, this equation is used to determine how the effects of a blast diminish with distance and the size of the explosive charge. As the scaled distance Z increases, the impact of the blast decreases. This is due to the cubic root relationship with the weight of the explosive charge.

Figure 7: Variation of blast pressure with distance

Boundary Condition

At height of 4 feet above the deck explosion occur as a result of this event bridge's main span is loaded with blast charge, as shown in figure 7. Assumed blast wave dispersion angle is 45° and wave dispersion range restricted to 10 m by 5.46 m as shown in figure 8. At the Centre of the span by using area tributary method, the uniformly distributed load is applied. The blast pressure induced in cable-stayed bridge's deck is 28.68 kPa. at the starting of the span.

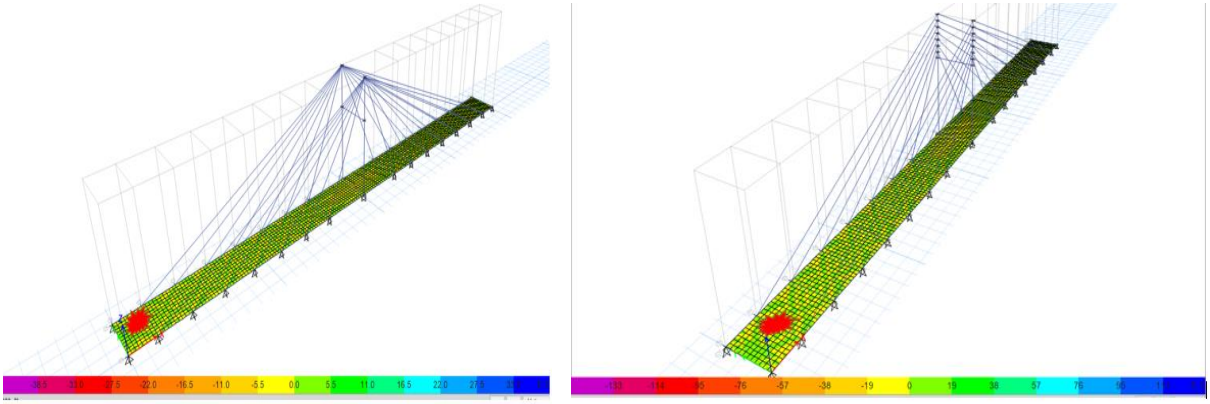

Radial H Type Fan H types

Figure 8: Blast loading location on Radial and Fan type cable-stayed bridges

The table 3 provides critical information regarding the application of blast loading on the deck of a bridge. Blast loading, which involves the sudden release of energy, can exert significant pressures on structures, including bridges, posing a challenge for their design and resilience. The data in the table presents the reflected pressure (Pso) in kilopascals (kPa) and the time of arrival of the blast wave (ta) in seconds for various scenarios.

The first entry in the table shows a reflected pressure of 15.50 kPa arriving at 0.0155 seconds (or 15.5 milliseconds) after the blast. This indicates an extremely rapid increase in pressure on the bridge deck. Subsequent entries detail decreasing pressures with corresponding arrival times: 4.80 kPa at 0.0048 seconds, 3.20 kPa at 0.0032 seconds, 2.10 kPa at 0.0021 seconds, 1.88 kPa at 0.0019 seconds, and 1.20 kPa at 0.0012 seconds.

These values are crucial for engineers and designers tasked with ensuring the structural integrity of the bridge under blast conditions. Understanding the timing and magnitude of these pressures helps in devising strategies to reinforce the bridge against such dynamic loads.

Table 3: Blast load and Time of arrival

Sr. No	Reflected Pressure, Pso (kPa)	Time of arrival of blast wave t_a (sec)
1	15.50	0.0155
2	4.80	0.0048
3	3.20	0.0032
4	2.10	0.0021
5	1.88	0.0019
6	1.20	0.0012

Figure 8 shows that location of blast load at starting of bridge main span and Table 3 shows main span experience a maximum pressure. Cables of stay bridge attached to the bridge's girder always subjected to tensile forces but ultimate tensile force developed due to the blast load in cables under their permissible limits hence there is no loss of cables. Table 4 & 5 shows the ultimate tension developed in radial type and Fan type cable arrangements.

Table 4: Blast load and Ultimate tension in cables

Radial H Type		
Cable	**Blast load (Pa)**	**Ultimate tension in cable (N)**
1	15500	4532.96
2	4800	3519.725
3	3200	2627.92
4	2100	1876.67
5	1880	1264.5
6	1200	783.19

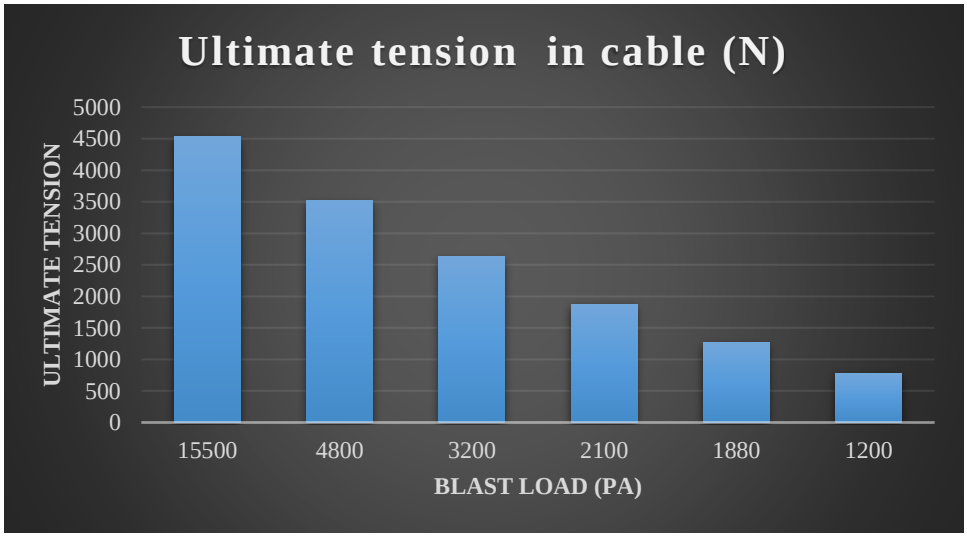

Figure 9: Blast loading vs ultimate tension in Radial type cable arrangement

The blast loads applied on a bridge deck, correlating them with the resulting ultimate tension in cables, reveals a crucial relationship in structural engineering. As the blast load increases, the ultimate tension in the cables also rises, demonstrating the bridge's deck dynamic behavior against reducing magnitude of explosive forces. For instance, at an initial blast load of 15,500 Pa, the ultimate tension in the cables reaches 4532.96 N. This trend continues with subsequent load reductions, such as at 4800 Pa resulting in 3519.725 N, 3200 Pa leading to 2627.92 N, and so forth. The data indicates a proportional relationship, where higher blast loads lead to greater cable tensions, showcasing the bridge deck's ability to resist and distribute these forces effectively. This information is invaluable for engineers designing structures to withstand potential blast events, ensuring safety and structural integrity under extreme conditions.

Table 5: Blast load and Ultimate tension in cables

Fan H Type		
Cable	**Blast load (Pa)**	**Ultimate tension in cable (N)**
1	15500	4535.22
2	4800	3484.15
3	3200	2559.88
4	2100	1783.81
5	1880	1152.73
6	1200	673.27

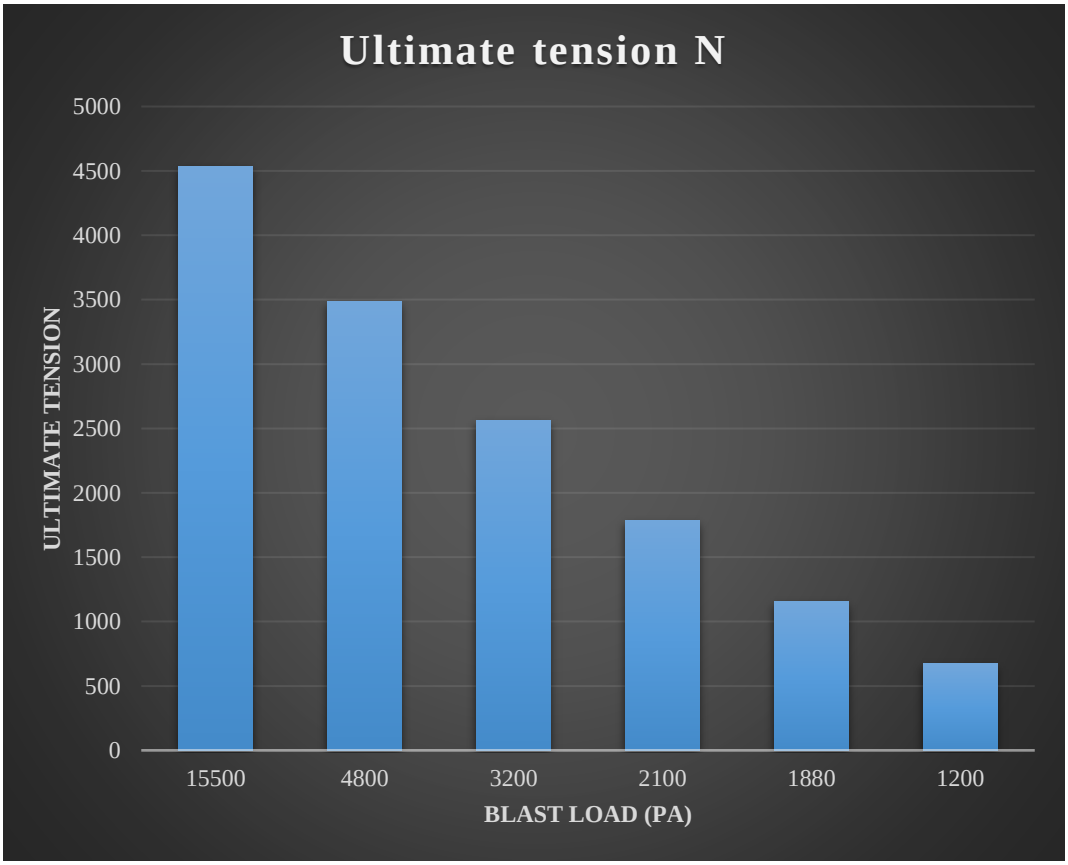

Figure 10: Blast loading vs ultimate tension in Fan type cable arrangement

The blast load (in Pascal's) applied on a bridge deck at various levels and the resulting ultimate tension in a cable (in Newton). As the blast load increases from 1200 Pa to 15,500 Pa, the ultimate tension in the cable increases from 673.27 N to 4535.22 N. This graph show a positive correlation between the tension in cable and blast load intensity. When the blast load is lower, such as 1200 Pa, the tension remains relatively low. However, as the blast load intensifies, so does the tension in the cable, reaching its maximum at 15,500 Pa. This data is crucial for engineers

designing bridge structures to withstand blast loads, as it demonstrates how increasing blast forces directly impact the tension and stresses experienced by critical components like cables.

Table 6: Comparison

Cable	Blast load (pa)	Radial H ultimate tension In Cable (N)	Fan H ultimate tension in Cable (N)
1	15500	4532.96	4535.22
2	4800	3519.725	3484.15
3	3200	2627.92	2559.88
4	2100	1876.67	1783.81
5	1880	1264.5	1152.73
6	1200	783.19	673.27

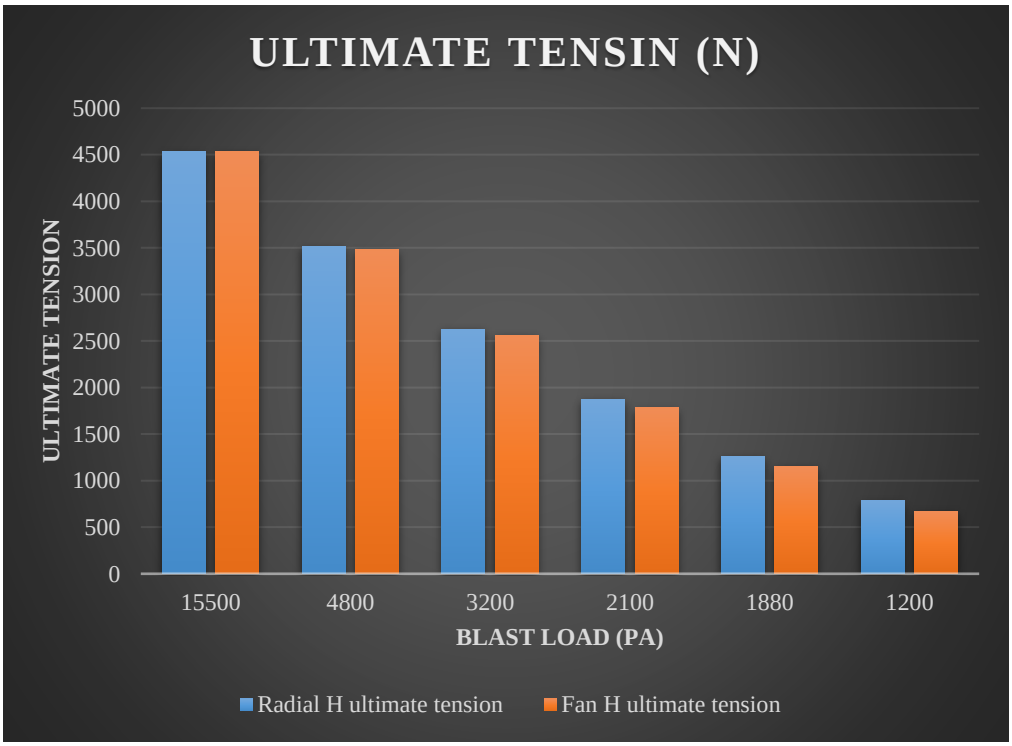

Figure 11: Comparison of ultimate tension in fan and radial arrangements

The comparison of blast loads applied to the bridge deck at various positions reveals a direct correlation with the ultimate tensions in the cables. As the blast load (pa) increases from 1200 to 15500, both the Radial H and Fan H ultimate tensions in the cables show a corresponding increase. This suggests that higher blast loads result in greater tension forces experienced by the cables supporting the bridge deck. For instance, at the highest blast load of 15500, the Radial H ultimate tension reaches 4532.96 N, while the Fan H tension hits 4535.22 N. Conversely, lower blast loads like 1200 pa correspond to lower tensions, with Radial H at 783.19 N and Fan H at 673.27 N. This data underscores the critical role of cables in bearing and distributing forces during blast events, indicating a need for designs that can withstand varying blast intensities.

Displacement

Displacement values in the X direction for a fan-shaped and radial H-type bridge deformations of deck.

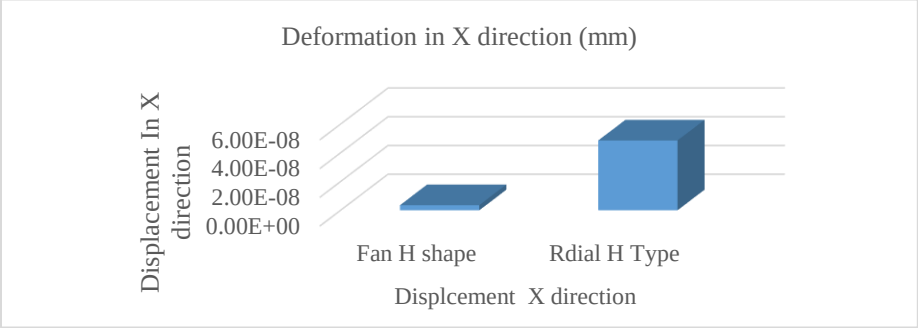

Figure 12: Deformation in x-direction

The given displacement values in the X direction for a fan-shaped radial H-type structure represent infinitesimal deformations, with the first value being 3.57E-09 and the second 4.86E-08. These numerical expressions, in scientific notation, signify extremely small displacements along the X-axis. Such minuscule deformations are typical in structural analysis, indicating the slight movement of the structure under applied loads or environmental conditions. While seemingly negligible, accurate measurement and interpretation of displacements are crucial in assessing structural stability, ensuring safety, and informing design modifications to optimize performance and mitigate potential risks or failures.

Story Drift y direction

The story drift of a bridge is a critical consideration in its design and safety. Imagine a bridge, gracefully spanning a river, its steel girders and concrete pillars standing like sentinels against the horizon. Beneath its majestic appearance lies a complex engineering marvel, where each inch matters. Story drift refers to the horizontal displacement or movement between adjacent levels or stories of a bridge structure during dynamic events, such as seismic activity or strong winds. It's a measure of how much the various parts of the bridge shift relative to each other.

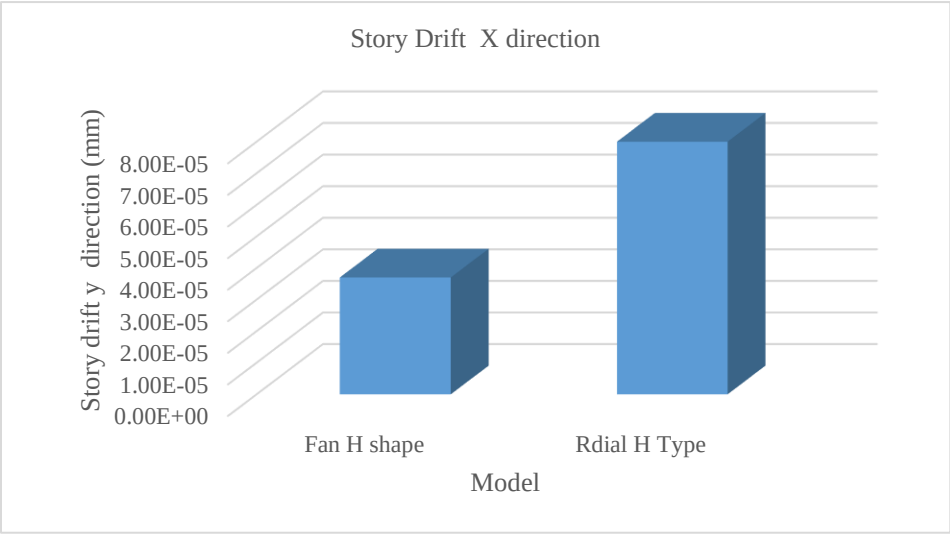

Figure 13: Story drift in X-direction

The provided data pertains to the story drift in the X direction for a fan-shaped radial H-type structure, with values of 3.70E-05 and 8.00E-05. These figures, expressed in scientific notation, indicate the lateral displacement or movement experienced by the structure at different levels or stories. In this context, the numerical values represent relatively small but discernible displacements along the Y-axis. Story drift is crucial in assessing the overall stability and integrity of a building, especially during seismic events or other dynamic loads. Accurate measurement and analysis of story drift inform engineers about potential structural vulnerabilities, aiding in the implementation of appropriate reinforcement or design adjustments to enhance structural resilience and safety.

Story Force Bottom

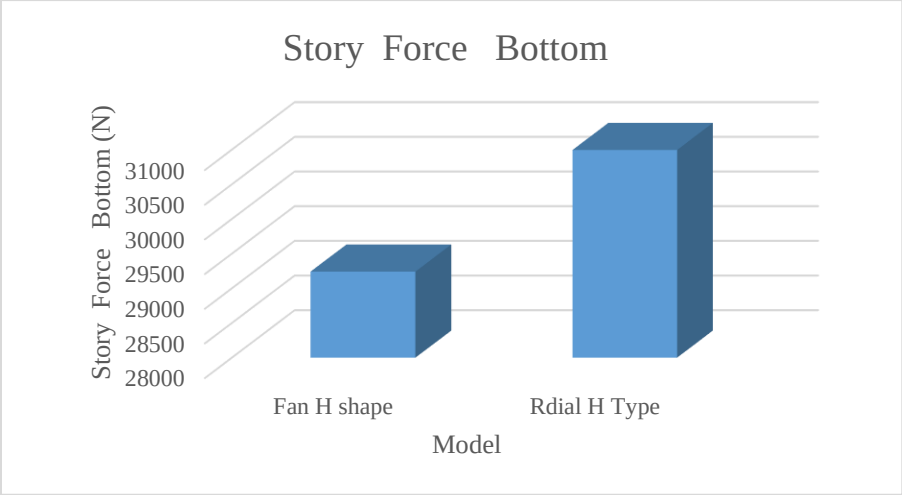

Figure 14: Forces at bottom

The given data presents the story force at the bottom level of a fan-shaped radial H-type structure, with values of 29240.7459 and 30994.9125. These numerical figures represent the magnitude of the force exerted on the structure at the lowest part, typically arising from applied loads such as gravity, seismic forces, or wind. In this context, the values signify the intensity of the forces acting on the structural elements, measured in units such as pounds or newtons. Analysis of story forces is vital in structural engineering to ensure that the components can adequately withstand the imposed loads, thereby guaranteeing the stability and safety of the entire structure. Comparing these values aids engineers in assessing load distribution and determining if any structural modifications or reinforcements are necessary to meet safety standards and design requirements.

Time Period

Time periods associated with different modes of vibration for two types of structures: fan-shaped and radial H-type. Each mode represents a distinct pattern of vibration or oscillation exhibited by the structures when subjected to dynamic loads, such as seismic events, blast load or wind forces. The time periods, measured in seconds, indicate the duration of one complete cycle of vibration for each mode. Generally, higher modes correspond to shorter time periods, signifying more rapid oscillations or higher frequencies of vibration. Engineers use this information to analyze the dynamic behavior of structures and assess their response to external forces, aiding in the design and optimization of structural systems for enhanced stability and performance under various loading conditions.

Table 7: Time Period

Time period (Sec)		
Mode	Fan H shape	Radial H Type
1	10.179	10.924
2	4.126	5.424
3	0.186	0.083
4	0.186	0.083
5	0.009	0.009
6	0.009	0.009
7	0.008	0.008
8	0.008	0.008
9	0.007	0.007
10	0.007	0.007
11	0.007	0.007
12	0.007	0.007

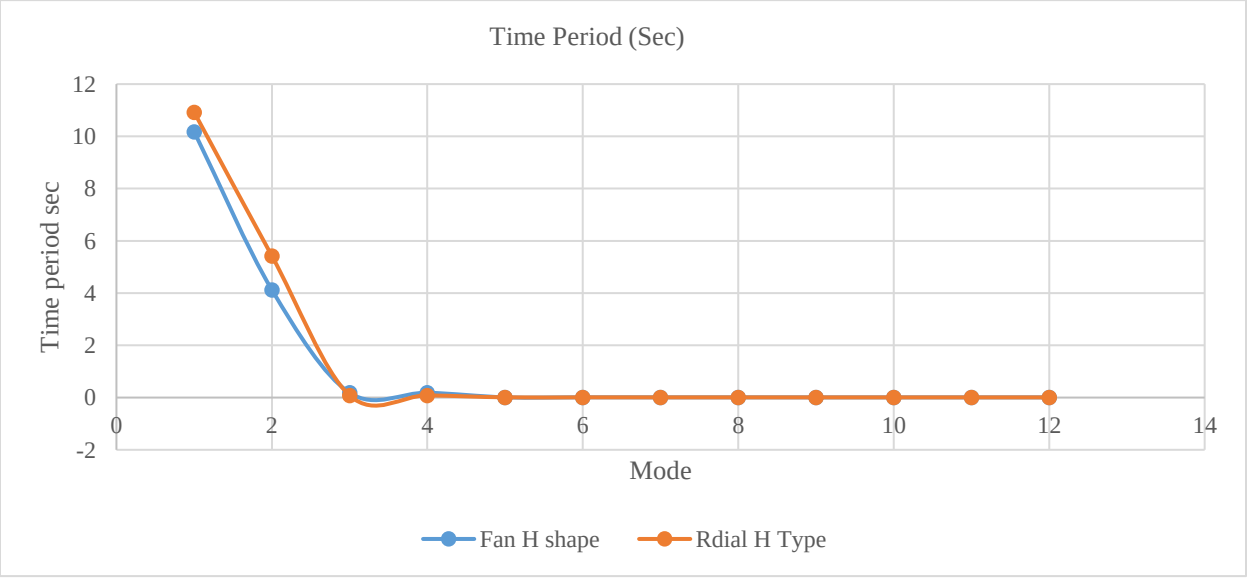

Figure 15: Comparison curve for time period

Frequency

Mode shape and natural frequency of any system depends on the material and geometrical properties of the system and independent of applied dynamic load. However, the dynamic response of structure depends on natural frequency and mode shapes as well as applied load

Table 10: Frequency

Frequency Hz		
Mode	Fan H shape	Radial H Type
1	0.098	0.092
2	0.242	0.184
3	5.379	12.027
4	5.379	12.027
5	112.533	112.533
6	112.533	112.533
7	129.911	129.911
8	129.911	129.911
9	146.204	146.204
10	146.204	146.204
11	146.227	146.227
12	146.227	146.227

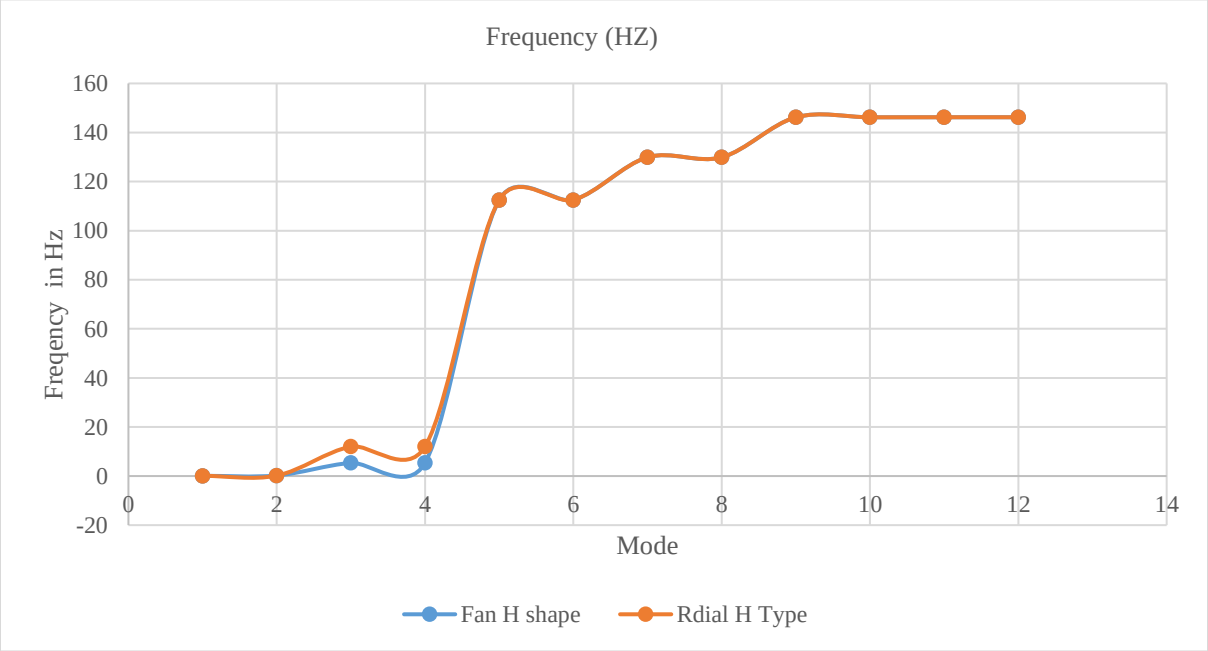

Figure 16: Frequency comparison curve

The presented data illustrates the frequencies, measured in Hertz (Hz), corresponding to different vibration modes for fan-shaped and radial H-type structures. Each mode represents a distinct pattern of vibration exhibited by the structures when subjected to dynamic loads. The frequency values indicate the number of complete oscillations or cycles per second for each mode. Higher mode numbers generally correspond to higher frequencies, reflecting more rapid

oscillations or vibrations. Engineers utilize this information to analyze the dynamic response of structures to external forces such as seismic events or wind loads, aiding in the assessment of structural stability and performance. Notably, the frequencies for each mode remain consistent across both fan-shaped and radial H-type structures, emphasizing the similarity in their dynamic characteristics

5. Conclusion

In this study comparing the progressive collapse behavior of cable-stayed bridges, various combinations of cable arrangements and pylon geometries were examined using the ETAB Finite Element Method (FEM) program under static loading conditions. The analysis focused on dynamic response of cable bridge structure. The choice of materials, including M40 grade concrete for the pylon and box girder and steel for cables and tendons, adheres to specified properties ensuring structural integrity and performance. The bridge design, featuring two end spans with a single pylon, is influenced by an extensive study of cable-stayed bridges globally. ETAB modeling further refines the structural representation, incorporating dynamic interactions. The two cable arrangements— Fan, and Radial—are modeled for H-type pylons.

The study on the dynamic response and progressive collapse analysis of cable-stayed bridges subjected to blast loading offers valuable insights into the performance of Radial H and Fan H Type cables under varying blast loads. The comparison between these cable types reveals interesting findings regarding their ultimate tension capacities. Both Radial H and Fan H Type cables exhibit an increase in ultimate tension as the blast load intensifies. Across all blast loads tested, Radial H Type cables demonstrate slightly higher ultimate tensions compared to Fan H Type cables. For example, at a blast load of 15500 Pa, Radial H cables reach an ultimate tension of 4532.96 N, while Fan H cables reach 4535.22 N.

This consistent trend of Radial H cables showing marginally higher ultimate tensions than Fan H cables persists throughout the range of blast loads studied. Despite this difference, both cable types exhibit a similar pattern of increased tension resistance with higher blast loads. Engineers can leverage this data to make informed decisions based on their specific project requirements. Radial H cables may be preferable for applications demanding slightly higher tension capacities, while Fan H cables offer competitive performance and could be selected for their cost-effectiveness or other design considerations.

Additionally, the study provides data on displacement values in the X direction for a fan-shaped radial H-type structure. These values, such as 3.57E-09 mm and 4.86E-08 mm in scientific notation, represent infinitesimal deformations along the X-axis. While these displacements may appear negligible, they are crucial indicators of the structure's response to applied loads and environmental conditions. Accurate measurement and interpretation of these displacements are vital for assessing structural stability, ensuring safety, and guiding design modifications to optimize performance and mitigate potential risks or failures.

Furthermore, the study includes information on story drift in the Y direction for a fan-shaped radial H-type structure, with values like 3.70E-05 mm and 8.00E-05 mm in scientific notation. These figures represent the lateral displacement or movement experienced by the structure at different levels or stories along the Y-axis. Story drift is a critical parameter for evaluating overall stability and integrity, especially during seismic events or dynamic loads. Precise measurement and analysis of story drift help engineers identify potential structural vulnerabilities, enabling them to implement appropriate reinforcements or design adjustments to enhance structural resilience and safety.

This study also includes the time period, frequency of Radial H-type cable arrangement and Fan H-type cable arrangement. Trend showing marginal difference in time period and frequency at lower mode in both type of cable arrangements. Despite this difference, both cable types exhibit a similar pattern of time period and frequency at higher modes.

References

[1]. H. L. Murphy, "Blast Loading on Structures," *J. Struct. Div.*, vol. 84, no. 7, 1958, doi: 10.1061/jsdeag.0000297.
[2]. D. Winget, K. Marchand, and E. Williamson, "Analysis and Design of Critical Bridges Subjected to Blast Loads," *J. Struct. Eng. - J STRUCT ENG-ASCE*, vol. 131, Aug. 2005, doi: 10.1061/(ASCE)0733-9445(2005)131:8(1243).
[3]. Adib K. Kanafani, *Blast-Resistant Highway Bridges: Design and Detailing Guidelines*. 2010. doi: 10.17226/22971.
[4]. C. M. Mozos and A. Aparicio, "Parametric study on the dynamic response of cable stayed bridges to the sudden failure of a stay, Part I: Bending moment acting on the deck," *Eng. Struct. - ENG STRUCT*, vol. 32, pp. 3288–3300, Oct. 2010, doi: 10.1016/j.engstruct.2010.07.003.
[5]. C. M. Mozos and A. C. Aparicio, "Parametric study on the dynamic response of cable stayed bridges to the sudden failure of a stay, Part II: Bending moment acting on the pylons and stress on the stays," *Eng. Struct.*, vol. 32, no. 10, pp. 3301–3312, 2010, doi: https://doi.org/10.1016/j.engstruct.2010.07.002.
[6]. Y. Zhou and S. Chen, "Numerical investigation of cable breakage events on long-span cable-stayed bridges under stochastic traffic and wind," *Eng. Struct.*, vol. 105, pp. 299–315, Dec. 2015, doi: 10.1016/j.engstruct.2015.07.009.
[7]. Ł. Mazurkiewicz, J. Malachowski, and P. Baranowski, "Blast loading influence on load carrying capacity of I-column," *Eng. Struct.*, vol. 104, pp. 107–115, Dec. 2015, doi: 10.1016/j.engstruct.2015.09.025.
[8]. Blue Ribbon Panel on Bridge and Tunnel Security, "Recommendations for bridge and tunnel security. American Association of State Highway and Transportation Officials (AASHTO)," *Transp. Secur. Task Force*, no. September, 2003, [Online]. Available: https://www.fhwa.dot.gov/bridge/security/brp.pdf
[9]. J. Son and H.-J. Lee, "Performance of cable-stayed bridge pylons subjected to blast loading," *Eng. Struct.*, vol. 33, pp. 1133–1148, Apr. 2011, doi: 10.1016/j.engstruct.2010.12.031.
[10]. H. Hao and E. Tang, "Numerical simulation of a cable-stayed bridge response to blast loads, Part II: Damage prediction and FRP strengthening," *Eng. Struct.*, vol. 32, pp. 3193–3205, Oct. 2010, doi: 10.1016/j.engstruct.2010.06.006.
[11]. Y. Pan, C. E. Ventura, and M. M. S. Cheung, "Performance of highway bridges subjected to blast loads," *Eng. Struct.*, vol. 151, pp. 788–801, 2017, doi: https://doi.org/10.1016/j.engstruct.2017.08.028.
[12]. W. F. Cofer, D. S. Matthews, and D. I. McLean, "Effects of blast loading on prestressed girder bridges," *Shock Vib.*, vol. 19, no. 1, pp. 1–18, 2012, doi: 10.3233/SAV-2012-0612.
[13]. S. Farahmand-Tabar and M. Barghian, "Seismic assessment of a cable-stayed arch bridge under three-component orthotropic earthquake excitation," *Adv. Struct. Eng.*, vol. 24, no. 2, pp. 227–242, Aug. 2020, doi: 10.1177/1369433220948756.
[14]. S. Farahmand-Tabar, M. Barghian, and M. Vahabzadeh, "Investigation of the Progressive Collapse in a Suspension Bridge Under the Explosive Load," *Int. J. steel Struct.*, vol. 19, pp. 2039–2050, Aug. 2019, doi: 10.1007/s13296-019-00263-x.
[15]. S. Farahmand-Tabar and M. Barghian, "Response control of cable-stayed arch bridge using modified hanger system," *J. Vib. Control*, vol. 26, pp. 2316–2328, Apr. 2020, doi: 10.1177/1077546320921635.
[16]. C. D. Tetougueni and P. Zampieri, "Structural response of cable-stayed bridge subjected to blast load," *Procedia Struct. Integr.*, vol. 18, pp. 765–774, 2019, doi: https://doi.org/10.1016/j.prostr.2019.08.225.

[17]. P. Shukla and C. K. Modhera, "Dynamic Response of Cable Stayed Bridge Pylon Subjected to Blast Loading," 2015, pp. 449–460. doi: 10.1007/978-81-322-2190-6_38.

[18]. S. K. Hashemi, M. A. Bradford, and H. R. Valipour, "Dynamic response of cable-stayed bridge under blast load," *Eng. Struct.*, vol. 127, pp. 719–736, 2016, doi: https://doi.org/10.1016/j.engstruct.2016.08.038.

[19]. M. Domaneschi *et al.*, "Collapse analysis of the Polcevera viaduct by the applied element method," *Eng. Struct.*, vol. 214, p. 110659, 2020, doi: https://doi.org/10.1016/j.engstruct.2020.110659.

[20]. M. Domaneschi, G. Cimellaro, and G. Scutiero, "Disproportionate collapse of a cable-stayed bridge," *Proc. Inst. Civ. Eng. - Bridg. Eng.*, vol. 172, pp. 1–39, Nov. 2018, doi: 10.1680/jbren.18.00031.

[21]. G. Gholipour, C. Zhang, and A. Mousavi, "Nonlinear numerical analysis and progressive damage assessment of a cable-stayed bridge pier subjected to ship collision," *Mar. Struct.*, vol. 69, p. 102662, Sep. 2020, doi: 10.1016/j.marstruc.2019.102662.

[22]. E. Tang and H. Hao, "Numerical simulation of a cable-stayed bridge response to blast loads, Part I: Model development and response calculations," *Eng. Struct.*, vol. 32, pp. 3180–3192, Oct. 2010, doi: 10.1016/j.engstruct.2010.06.007.

[23]. R.-B. Deng and J. Xianlong, "Numerical simulation of bridge damage under blast loads," *WSEAS Trans. Comput.*, vol. 8, Sep. 2009.